Available online at www.sciencedirect.com
SCIENCE DIRECT
Scripta Materialia 54 (2006) 1715–1719
Scripta MATERIALIA
www.actamat-journals.com

Intermixing criteria for reaction synthesis of Ni/Al multilayered microfoils

Hee Y. Kim [a], Dong S. Chung [b], Soon H. Hong [a,*]

[a] Department of Materials Science and Engineering, Korea Advanced Institute of Science and Technology, 373-1 Guseong-dong, Yuseong-gu, Daejeon 305-701, South Korea
[b] Department of Materials, Daegu Polytechnic College, 1495 Pyungri-dong, Seo-gu, Daegu 681-280, South Korea

Received 23 June 2005; accepted 8 December 2005
Available online 25 January 2006

Abstract

Intermixing criteria are proposed for determining the microstructure of the reaction products during the reaction synthesis of Ni/Al multilayered microfoils. The critical thickness and thickness ratio for the formation of monolithic intermetallic depend on the conductive heat loss through the Ni layer and are verified by analytical thermophysical modeling.

Keywords: SHS; Multilayers; Nickel aluminides; Intermixing; Finite element analysis

1. Introduction

The reaction synthesis technique for intermetallics involves both a self-propagating high-temperature synthesis (SHS) mode and a thermal explosion (TE) mode depending on the shape, size, and thermophysical properties of the constituent phases. Recently, in situ composites [1–4] and monolithic intermetallic [5] have been successfully manufactured by alternately stacking commercial elemental foils, such as Ni, Ti, Nb, Fe, and Al, in the TE mode. With nano-multilayer reactants, the spontaneous SHS reaction can achieve very high temperatures, which will melt the surrounding materials, and can be used to join electronic parts [6,7]. In the TE reaction mode using micro-sized element foils, the geometry and thermophysical properties of each element foil will obviously determine the final microstructure.

Atzmon [8] reported that the dependence of the ignition temperature for Ni/Al diffusion couples on the heating rate was a result of interfacial barriers based on Gosele's results [9]. His model neglected the thermal gradient and melting of the element foil. Zhu et al. [10,11] studied the reaction synthesis of multilayered Ni and Al foils in the TE mode and reported that the reaction started at the melting point of Al independent of the thickness of the Ni foil. Jayaraman et al. [12] performed thermophysical modeling of the reaction front in Ni/Al nano-multilayers for application as joining materials and concluded that the radiative heat losses from the reactant had a much smaller effect on reaction propagation than did the conductive heat losses through each layer.

As stated above, the microstructure of the product in the TE mode reaction of Ni/Al multilayered microfoils is determined by the thermophysical properties of the element foil, but their effects on microstructure have not been clarified in micro-sized multilayers. Most research has focused on the reaction stage, and the effect of heat conduction through the element foils has been neglected. Therefore, we conducted a thermophysical analysis of Ni/Al multilayered microfoils using experimental values for the time–temperature profile during the reaction.

* Corresponding author. Tel.: +82 42 869 3327; fax: +82 42 869 3310.
E-mail address: shhong@kaist.ac.kr (S.H. Hong).

1359-6462/$ - see front matter
doi:10.1016/j.scriptamat.2005.12.032

2. Experimental procedures

2.1. Reaction synthesis of Ni/Al multilayered microfoils

Commercially pure (⩾99.0%) nickel (12, 25, 30, 50, 75, and 100 μm; Nilaco Co.) and aluminum (10, 18, 20, 25, 50, and 100 μm; Goodfellow Co.) foils were prepared. These foils were cut into 20 × 20-mm squares and were cleaned in an ultrasonic acetone bath for 10 min. The multilayer combinations shown in Table 1 were stacked alternatively in 2-mm thicknesses. The stacked multilayers were placed in a vacuum hot-press under 10^{-2}–10^{-3} Torr. Thermocouples were embedded between the Ni and Al foils to measure the initiation of the reaction (T_{ig}) and the temperature increase (T_{ad}) during the reaction. Both ends of the stacked pile were insulated with zirconia felt (ZYF-100) to minimize the heat loss during the reaction and were pressed with a punch at 10 MPa. The stacked pile was diffusion bonded for 1 h at 600 °C to remove the reaction barrier. The diffusion-bonded specimens were heated to 750 °C and held at this temperature for 0.5–1 h, depending on the initial thickness ratio. No pressure was applied to the specimens during the reaction at 750 °C. The microstructure of the reaction product was observed using optical and scanning electron microscopy. The crystal structure and chemical composition of each constituent phase were analyzed using energy-dispersive spectroscopy and X-ray diffraction.

2.2. Thermophysical modeling

In order to analyze the heat transfer at the interface in the Ni/Al microfoils during the reaction, a simple heat equation is introduced [13]. Considering only a one-dimensional heat equation in the x-direction and assuming that the other directions are insulated thermally, then

$$\rho C_p \frac{\partial T}{\partial t} = \frac{\partial}{\partial x}\left(k\frac{\partial T}{\partial x}\right) + \dot{q} + q_{\text{rad}} \tag{1}$$

Table 1
Combinations of Ni/Al multilayered microfoils used in the reactions

Initial thickness (μm)		Thickness ratio (Ni/Al)	T_{ad} (°C)
Ni	Al		
12	10	1.2	>1370
20	10	2.0	–
20	18	1.1	–
25	10	2.5	–
30	10	3.0	–
30	25	1.2	1069
50	10	5.0	–
50	20	2.5	–
50	50	1.0	960
75	10	7.5	–
100	25	4.0	722
100	50	2.0	762
100	100	1.0	791

where ρ, C_p, $\dot{q}$, q_{rad} are the density, specific heat, heat generation rate, and radiative heat loss rate, respectively. The rate of heat loss owing to radiation, q_{rad}, is expressed as

$$q_{\text{rad}} = -\varepsilon\frac{2\sigma(T^4 - T_0^4)}{\lambda} = -h\frac{S}{V}(T - T_0) \tag{2}$$

where ε, σ, T_0, h, S, and V are the emissivity, Stefan–Boltzmann constant, heat transfer coefficient, surface area, and volume, respectively. As shown in Fig. 1, the z direction perpendicular to lamination is thermally insulated by zirconia and the heat is radiated only to the x and y directions parallel to lamination. In the x and y directions, the effective surface area from which the heat is radiated is very small compared to the total volume of sample, because the thickness of the product layer is calculated to 0.9–2.8 μm during heat generation by reaction synthesis. Therefore, q_{rad} during reaction synthesis is neglected in the x and y directions. q_{rad} is not so significant even in the nanometer range, in which the combined thickness (λ) is very small [12]. Here, the heat generation term is related to the rate at which the reaction progresses. This relationship introduces a new parameter, the heat of reaction. This quantity gives the magnitude of the heat liberated by the reaction:

$$\dot{q} = \rho H\frac{\partial C}{\partial t} = \rho H\frac{\partial\left(\frac{x^c}{\lambda}\right)}{\partial t} = \frac{\rho H}{\lambda}\frac{\partial x^c}{\partial t} \tag{3}$$

The growth rate of the product layer, $\partial x^c/\partial t$, is given by [8]

$$\frac{dx^c}{dt} = \frac{G\widetilde{D}^c\Delta C^c\kappa}{\widetilde{D}^c + x^c\kappa} \tag{4}$$

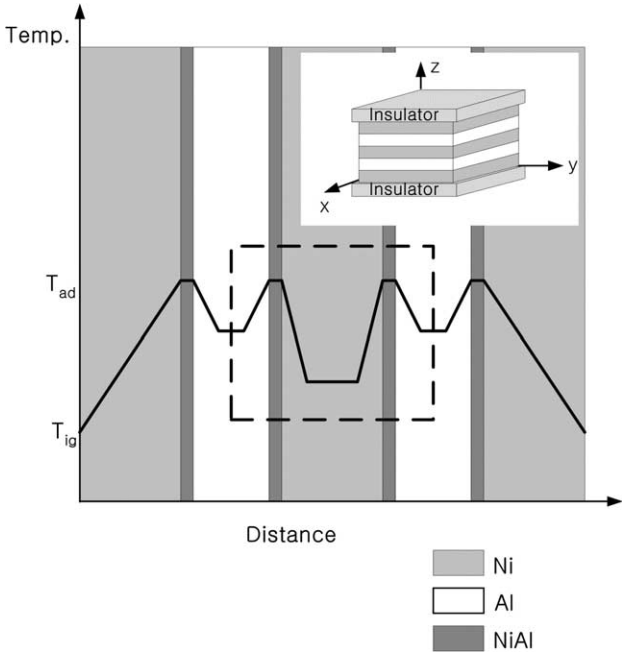

Fig. 1. Sample setup (inset) and schematic xz or yz plane used for transient thermal analysis during reaction synthesis of Ni/Al microfoils. Dotted box is symmetric element for finite element modeling.

where x^c, $\widetilde{D}^c$, G, ΔC^c, and κ are the instantaneous thickness of the compound layer, the interdiffusion coefficient in the compound, a composition variable related to the molar volume change, the solubility range of the compound at the given temperature, and the interfacial reaction constant, respectively. When the interfacial barrier can be ignored as a result of diffusion bonding before the reaction, as in our case, then

$$\frac{dx^c}{dt} \approx \frac{G\widetilde{D}^c\Delta C^c}{x^c} \tag{5}$$

Integrating Eq. (5), we get

$$x^c = \sqrt{2G\widetilde{D}^c\Delta C^c t} \tag{6}$$

If Eq. (3) is substituted into Eq. (2), then

$$\frac{dT}{dt} = \alpha\frac{\partial^2 T}{\partial x^2} + \frac{H}{C_p\lambda}\frac{\partial x^c}{\partial t} \tag{7}$$

where $\alpha = \kappa/\rho C_p$.

Eq. (7) is similar to the results deduced from Atzmon's model [8], except it introduces the conductive heat loss instead of the radiative heat loss. From previous results [12], the conductive heat losses are thought to be higher in our experimental conditions. These governing equations were simulated using commercial finite element modeling (FEM) software. The plane 55 element of the ANSYS thermal module was used for two-dimensional transient thermal analysis. This element has four nodes with a single degree of freedom, temperature, at each node. A transient system in a semi-infinite dimension is assumed for time-step processing. Assuming symmetry in the x-direction, the geometries for Ni layers with thicknesses of 5, 10, 20, 30, and 50 μm at a 1:1 thickness ratio are created as shown in Fig. 1. Reported thermophysical data [14] for the reactant and product were used as input values for the simulation, and other unknown values were based on the experimental results, as explained below.

3. Results and discussion

3.1. Effect of thickness and thickness ratio on microstructure

Fig. 2 shows the microstructure of intermetallic/metal microlaminate and monolithic intermetallics obtained from the Ni/Al multilayered microfoils. While the microlaminates have a layered structure of Ni_3Al, $Ni_{0.58}Al_{0.42}$, and Ni after heat treatment at 950 °C, the monolithic intermetallic consisting of white (Ni_3Al) and black ($Ni_{0.58}Al_{0.42}$) phases do not contain a pure Ni phase owing to the complete consumption of the Ni layer. When reactions for every combination listed in Table 1 are performed, it is confirmed that there are criteria for complete intermixing which result in monolithic intermetallic formation below a critical thickness and thickness ratio. Fig. 3 summarizes the product type depending on the thickness and thickness ratio. The hatched area shows the possible range for monolithic intermetallic formation. When the combined thickness (λ) is low and the thickness ratio is 1:1, a monolithic intermetallic forms, as shown in Fig. 2. Intermixing occurs below this critical combined thickness (λ_c).

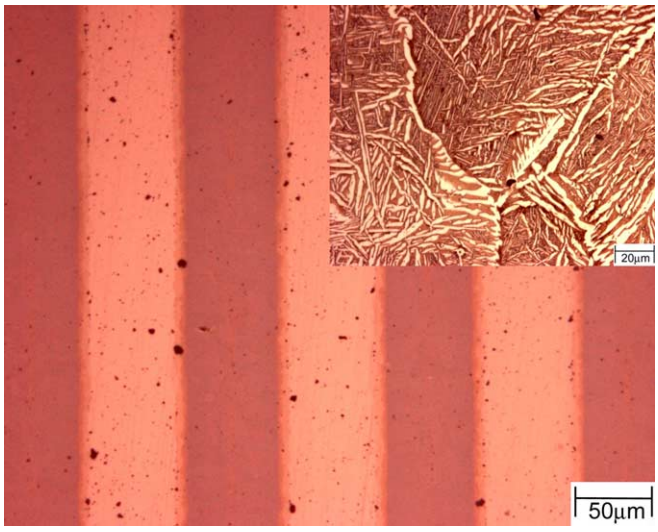

Fig. 2. Microstructures of intermetallic/metal microlaminate (initial $t_{Ni} = 100$ μm) obtained by reaction synthesis at $t_{Ni}/t_{Al} = 1{:}1$. The inset shows a monolithic intermetallic (initial $t_{Ni} = 20$ μm).

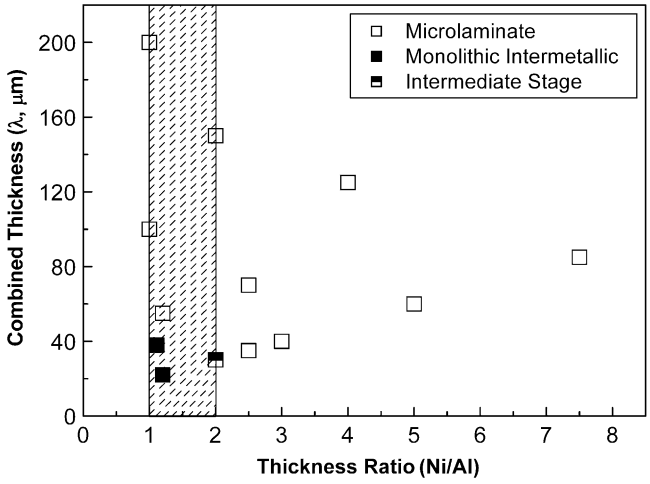

Fig. 3. Diagram summarizing the microstructure type with respect to the thickness and the thickness ratio.

Fig. 4 shows the time–temperature curves for various combined thicknesses. Below a combined thickness of 40 μm, the adiabatic temperature increases above 1370 °C, which is the limit of the K-type thermocouple used to measure temperature. The temperature is presumed to approach the theoretical adiabatic temperature (T_{ad}) for NiAl [15]. The ignition temperature (T_{ig}) is similar for all combinations because it is related to the melting of aluminum and the diffusion barrier. The latent time is mainly related to the thickness of aluminum, while the adiabatic temperature is related to heat conduction through the

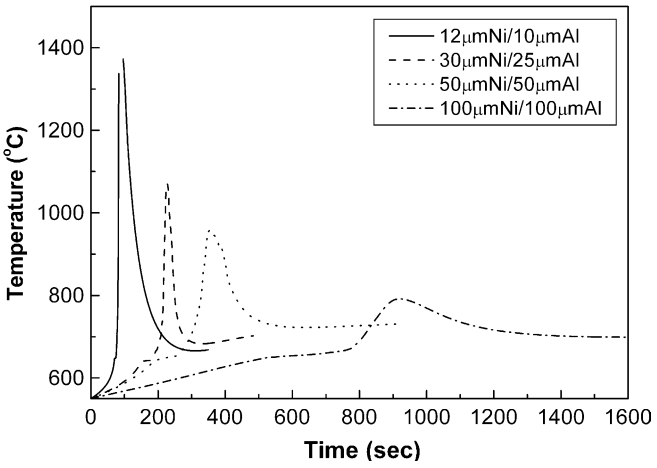

Fig. 4. Time–temperature curves for various combined thicknesses (λ).

nickel layer, and T_{ad} decreases as the nickel layer increases. Thus, complete intermixing is caused by the combined effects of thickness, thickness ratio, and the thermophysical properties of the metal and intermetallic layer.

3.2. Effect of conductive heat loss through the Ni layers

Intermixing of Ni and Al consists of complex reactions such as dissolution of Ni in liquid Al, precipitation of solid NiAl and Ni_3Al in supersaturated Ni/Al solution, and dissolution of the intermetallic. The adiabatic temperature ranges from 1300 to 1800 °C [11]. In our model to investigate the effect of thickness and thickness ratio on microstructure, the first step of intermixing of Ni and Al is regarded as dissolution of Ni in liquid Al. Data on the growth rate of the intermetallic layer is required to simulate the transient behavior during the reaction of multilayered microfoils using Eq. (7). Nakamura et al. [16] reported the interdiffusion coefficients of the NiAl phase over a wide temperature range from 1073 to 1773 K. In our case, the diffusivity data for NiAl at 1773 K were applied because the measured temperature exceeded 1643 K and the maximum temperature should exceed the melting temperature (1728 K) of Ni for intermixing to occur. The ΔC^c is the solubility range for the intermetallic at a given temperature, and G is given by [8,9]

$$G = \Omega(1+\beta)^2\left(\frac{1}{\alpha-\beta}+\frac{1}{\beta-\gamma}\right) \tag{8}$$

where Ω is the atomic volume, α and γ represent the number of A atoms per B atom in the reactant, respectively, and β is the same number for the product. For NiAl, we assume $G = 4\Omega$ and that ΔC^c is very small, $0.01/\Omega$. Then, the NiAl growth rate calculated using Eq. (6) is 0.894 μm at 10 s when intermixing occurs at $\lambda = 40$ μm, as shown in Fig. 4. This result is reasonable because NiAl grew to 20 μm over 1 h as the microlaminate was post-heat-treated at 1273 K in our experiment. Given the reported material properties [14], the boundary conditions based on the experimental results are assumed to be as follows: thickness ratio = 1:1, Ni thicknesses = 5, 10, 20, 30, or 50 μm, $T_{ig} = 660$ °C, and $T_{ad} = 1500$ °C in the semi-infinite dimension. The symmetric geometry for the calculation is shown in Fig. 1 and the results for the unit cell enclosed by the dotted line are displayed. The typical transient thermal gradient at $t_{Ni} = 5$ μm thickness is shown in Fig. 5. When t_{Ni} increases, the temperature at the center of the Ni layer increases very slowly owing to the lower thermal conductivity of Ni than that of Al. For complete intermixing to occur, the temperature at the center of the Ni layer should increase to $T_{m,Ni} = 1455$ °C before heat dissipation. Fig. 6 shows the time required to arrive at $T_{m,Ni} = 1455$ °C. As the Ni thickness increases, the time to $T_{m,Ni}$ increases markedly. The experimental values and simulated results for the temperature at the center of the Ni layer are compared in Fig. 7. As the single-layer thickness ($\lambda/2$) increases, the time increases sharply, so that a Ni layer thicker than 10 μm cannot approach $T_{m,Ni}$ at all. The experimental T_{max} measured from Fig. 4 was also compared with the calculated values, and the times to reach T_{max} were similar. As a result, heat conduction through the Ni layer determines

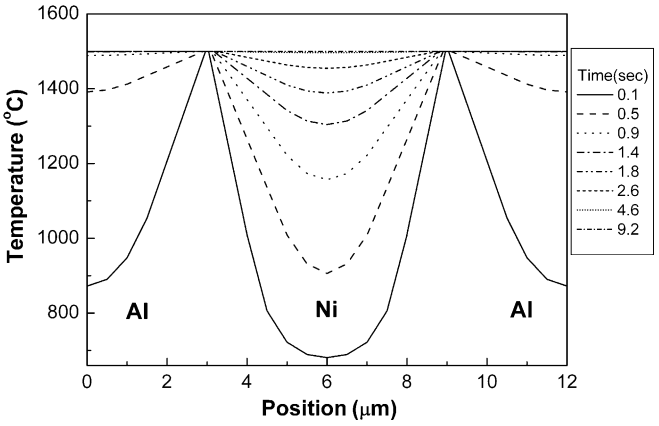

Fig. 5. Transient thermal gradient during the formation of NiAl at $t_{Ni} = 5$ μm.

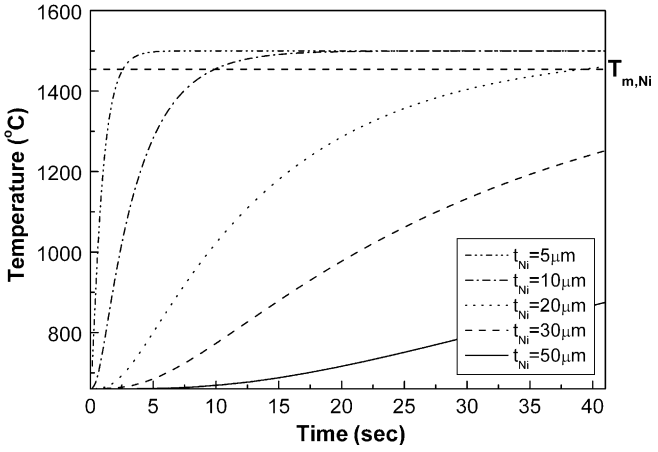

Fig. 6. Time required to arrive at $T_{m,Ni} = 1455$ °C as a function of t_{Ni}.

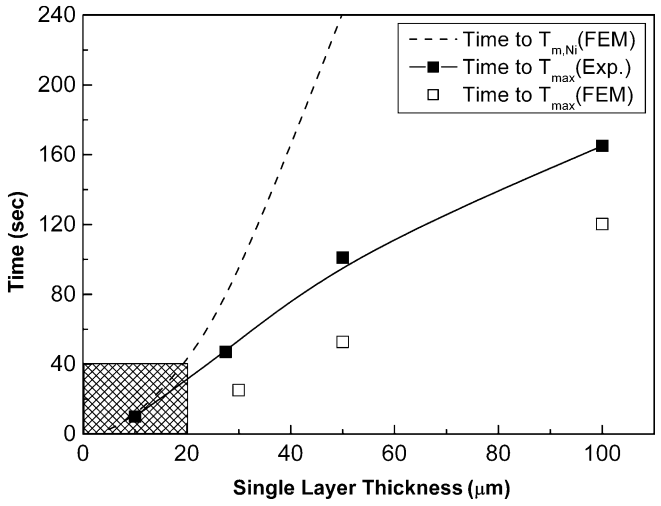

Fig. 7. Comparison of the FEM-simulated and experimental values of the times to $T_{m,Ni}$ and T_{max}.

the complete intermixing of Ni and Al, and the critical combined thickness, λ_c, is around 20 μm under our experimental conditions. If additional surrounding thermal insulation is used, it should be possible to precisely predict the critical combined thickness necessary for intermixing.

4. Conclusions

The microstructures created by the reaction synthesis in Ni/Al multilayered systems were divided into microlaminate and monolithic intermetallics, depending on the thickness and thickness ratio of microfoils. Thermal equations were formulated using the heat generated by the reaction of Ni/Al and the heat conduction through each layer. Finite element analysis results showed that the main heat loss during the reaction of Ni/Al was limited by conductive loss through the Ni layer, which has a lower thermal conductivity than the Al layer. The simulated transient thermal responses behaved in a similar manner to the experimental curve.

Acknowledgement

This research was supported by the Korea Institute of Science and Technology Evaluation and Planning under contract M1-0105-00-0023.

References

[1] Kim HY, Chung DS, Hong SH. Mater Sci Eng A 2005;396:376.
[2] Alman DE, Dogan CP, Hawk JA, Rawers JC. Mater Sci Eng A 1995;192:624.
[3] Alman DE, Rawers JC, Hawk JA. Metall Mater Trans A 1995;26:589.
[4] Bloyer DR, Rao KTV, Ritchie RO. Mater Sci Eng A 1996;216:80.
[5] Alman DE, Dogan CP. Metall Mater Trans A 1995;26:2759.
[6] Swiston Jr AJ, Hufnagel TC, Weihs TP. Scripta Mater 2003;48:1575.
[7] Weihs TP, Reiss M. US Patent 6,534,194; 2003.
[8] Atzmon M. Metall Trans A 1992;23:49.
[9] Gosele U, Tu KN. J Appl Phys 1982;53:3252.
[10] Zhu P, Li JCM, Liu CT. Mater Sci Eng A 1997;239:532.
[11] Zhu P, Li JCM, Liu CT. Mater Sci Eng A 2002;329:57.
[12] Jayaraman S, Mann AB, Reiss M, Weihs TP. Combust Flame 2001;124:178.
[13] Geiger GH, Poirier DR. Transport phenomena in metallurgy. Reading, MA: Addison-Wesley; 1973. p. 290.
[14] Kubaschewski O, Alcock CB, Spencer PJ. Materials thermochemistry. 6th ed. Oxford: Pergamon Press; 1993. p. 257.
[15] Morsi K. Mater Sci Eng A 2001;299:1.
[16] Nakamura R, Takasawa K, Yamazaki Y, Iijima Y. Intermetallics 2002;10:195.